OBSERVATIONS OF DEFORMATION IN ORTHOPYROXENE-RICH SUBSAMPLE OF DIOGENITE NORTHWEST AFRICA 1877. A. L. Fagan[1], L. Turner[1], C. Waters-Tormey[1], and G. Casale[2], [1]Geosciences and Natural Resources Dept., Western Carolina University, Cullowhee, NC 28723 (alfagan@wcu.edu), [2] Dept. of Geological and Environmental Sciences, Appalachian State University, Boone, NC 28608.

Introduction: Diogenite meteorites are ultramafic rocks that are generally accepted to be from the deep crust or upper mantle of the differentiated asteroid 4 Vesta or one of the vestoids [e.g., 1-4]. Diogenites are typically orthopyroxenites (i.e., ≥90% orthopyroxene, [4]), although some harzburgites (i.e., equal amounts of olivine and Mg-rich orthopyroxene, [e.g., 5]) have been found. Northwest Africa (NWA) 1877 has been classified as an olivine-rich diogenite (i.e., harzburgitic, [6-7]) with subequal amounts of orthopyroxene and olivine along with minor Al-poor chromite, troilite, and Ni-free metal [6]; however, it has also been classified as an anomalous diogenite [e.g., 8].The magnesian silicate phases are compositionally similar to two olivine diogenites recovered from Antarctica, but distinct from one recovered from Morocco (NWA 1459, [7]), suggesting some compositional variation between the olivine-rich diogenite suite. Chromite from NWA 1877 has a higher Cr content than other olivine diogenites and lacks plagioclase, which suggests that it may originate as a deep primitive mantle material [7].

Examination of another olivine diogenite (NWA 5480) has yielded insight into the deformation history of the interior of Vesta; plastic deformation in solid state conditions early in the formation of the parent body has been suggested using chemical composition, modal mineralogy, texture, and olivine structural information [9], which has also been documented in two additional olivine-rich diogenites [10]. This style of deformation is suggested to have occurred due to "downwellings of lid material" and implies a geologically active body [9]. In order to continue to investigate the internal history of the diogenite parent body, we examine the petrography, chemistry, and structural orientation of mafic phases within a subsample of NWA 1877.

Sample Description: In contrast to previous descriptions of NWA 1877 as being olivine-rich, our split (purchased from R. Wesel in 2015) is completely devoid of olivine and therefore may be unrepresentative of the main sample. Instead, the sample is almost entirely composed of orthopyroxene (OPX) with several isolated chromite grains (up to ~100 x 200 μm) and small blebs of opaque phases. OPX grains range in size from <100 μm to nearly 1 mm and are mostly characterized by having expected low interference colors (Fig. 1). Several OPX grains are unique with bright blue interference colors; these grains tend to be located within a thin (~ 250 μm wide) zone of smaller, angular OPX grains without a defined grain shape fabric (see "Breccia Zone" in Fig. 1). Some OPX grains show patchy extinction indicating some shock damage as seen with the unbrecciated Tatahouine diogenite [4].

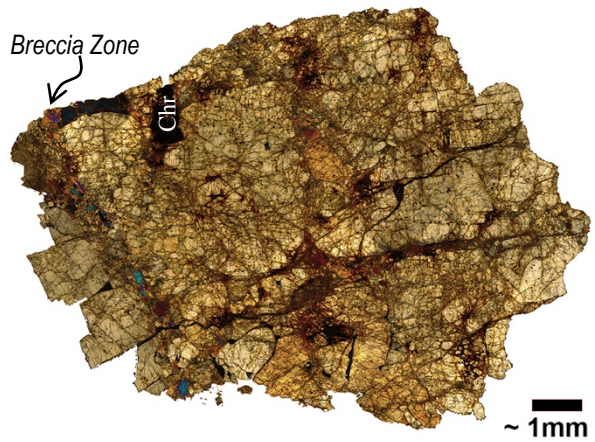

Fig. 1. Cross-polarized light mosaic of NWA 1877. OPX dominates the thin-section (first order interference colors up to second order blue) with one large chromite (Chr).

EMP & EBSD Methods: Major and minor elemental abundances of OPX and chromite were characterized using electron probe microanalysis (EPMA) via the Cameca SX 100 at the University of Tennessee; instrument settings were: 15 kV, 30nA, and on-peak count times of 30 sec. Natural and synthetic materials were employed as standards.

Crystal orientation measurements using electron backscatter diffraction (EBSD) were collected on a JEOL JSM-IT300 scanning electron microscope (SEM) equipped with a LaB6 filament and Oxford NordlysNano EBSD detector at Appalachian State University. Data were collected at 25 KeV accelerating voltage under low vacuum conditions of 30 Pa, 25 um step size, and a dwell time of 17 μs. Data were cleaned and maps were constructed using Inca and Mambo software applications from Oxford Instruments, and included single pixel wild-spike removal, and removal of intragrain single pixel zero solutions. EBSD measurements were taken from a potted butt from whence the thin-section was taken.

Results: *EPMA*. OPX grains show little variation in composition (En 74.4-75.2, Fs 23.4-24.3, Wo 1.3-1.5) across the thin-section and plot within the typical compositional range of diogenites [e.g., 4] (Fig. 2). The OPX Mg# [Mg/(Mg+Fe)*100] ranges 75.4 to 76.3, and the Fe/Mn ratio ranges 25.3 to 29.4. Chromite Mg# ranges 18.5 to 18.7 with Cr/(Cr+Al) ~0.86. These OPX

and chromite compositions are consistent with previously published data for NWA 1877 [7, 11].

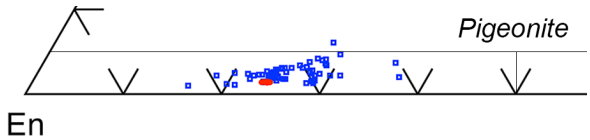

Fig. 2. Truncated pyroxene quadrilateral of NWA 1877 from this study (18 overlapping red dots) compared to OPX from other diogenites (blue squares, [4 and references therein]).

Preliminary EBSD. Diffraction patterns confirm that this subsample of NWA 1877 is predominantly OPX with some chromite and no olivine. Most of the OPX have the same orientation (brownish-red color, Fig. 3). However, OPX in the breccia zone (Figs. 2, 3) are distinctly green and purple in the EBSD map, which represents a large difference in orientation from the majority of the sample. OPX grains within the breccia zone tend to have similar orientations to each other (Fig. 3). In addition to the main breccia zone, several additional zones of angular brecciated material can be seen (Fig. 3).

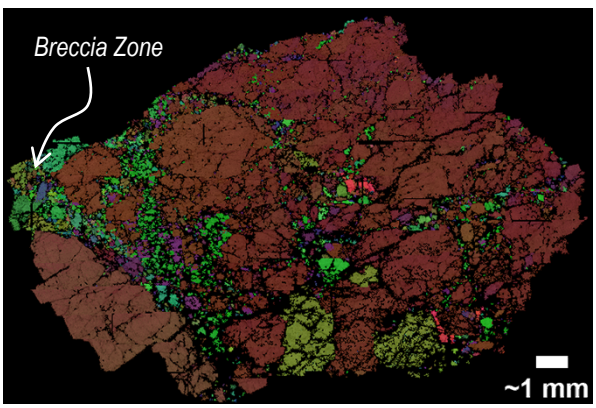

Fig. 3. EBSD map showing crystallographic orientations of constituent phases. Color corresponds to crystal orientation.

Discussion and Implications: Despite a clear distinction in the modal mineralogy between our split of NWA 1877 and those used to classify the sample as an olivine-rich diogenite, the similarity in chemical composition for the OPX and chromite [7, 11] suggest they are indeed from the same meteorite.

Although some studies have shown that minor and trace element compositions between different grains, and across a single large grain, in diogenites can be highly variable [e.g., 12-14], the minor element compositions across this sample show very little variation (e.g., Al_2O_3 0.34-0.39 wt%, TiO_2 0.02-0.06 wt%). The composition is consistent with previous work that has shown that NWA 1877 has similar mafic silicate compositions to some olivine-rich diogenites, but more Cr-rich chromite [7] suggestive of a more primitive nature. Our study shows that our subsample of NWA 1877 has OPX with similar Al and Ti content to Meteorite Hills (MET) 00436, an unbrecciated diogenite with similar large chromite grains, but the NWA 1877 OPX (Mg# 75.4 to 76.3) are more primitive than that of MET 00436 (Mg# 70 to 71, [15]). Moreover, the NWA 1877 chromite has a higher Mg# and lower Al_2O_3 content (~ 3.6 wt%) compared to MET 00436 [16].

The majority of our subsample is characterized by OPX with a single orientation (Fig. 3) and with homogeneous chemical signature (Fig. 2), therefore this suggests that most of the thin-section is dominated by a single OPX grain ~16 mm wide. In contrast, the finer-grained breccia zones (purple and green, Fig. 3) have different orientations, and yet similar chemical composition (Fig. 2) to the main grain. Such chemical homogeneity between grains across the sample suggests that the OPX formed in a chemically closed system and that the smaller grains may have originated as part of the main, coarse grain (i.e., "parent"). If so, some deformation must have occurred to cause the brecciation and preferred misalignment of OPX within the breccia zones. It is unclear at this time how this deformation compares to the solid-state, plastic deformation seen in olivine from NWA 5480 [9]; notably, the OPX in NWA 5480 shows no indication of solid-state plastic deformation [17]. More detailed EBSD analyses are required, particularly to ascertain the numerical relationship between the original orientation (i.e., that of the "parent" grain) and those of a different orientation (i.e., within the breccia zones).

References: [1] Pieters C.M. et al. (2005) *Asteroids, Comets, Meteors- Proceedings IAU Symp.*, **229**, 273-288. [2] Wasson J.T. (2013) *Earth Planet. Sci. Lett.*, **381**, 138-146. [3] McSween H.Y., Jr. et al. (2013) *Meteorit. Planet. Sci.*, **48**, 2090-2104. [4] Mittlefehldt D.W. (2015) *Chemie der Erde*, **75**, 155-183. [5] Beck A.W. and McSween H.Y., Jr. (2010) *Meteorit. Planet. Sci.*, **45**, 850-872. [6] Russell S.S. et al. (2004) Met. Bull. 88, *Meteorit., Planet. Sci.*, **39**, Supp. A215-A272. [7] Irving A.J. et al. (2005) *LPS XXXVI*, Abstract #2188. [8] McCausland P.J.A. et al. (2011) *Meteorit. Planet. Sci.*, **46**, 1097-1109. [9] Tkalcec B.J. et al. (2013) *Nature Geosci.*, **6**, 93-97. [10] Tkalcec B.J. and Brenker F.E. (2014) *Meteorit. Planet. Sci.*, **49**, 1202-1213. [11] Yamaguchi A. et al., (2011) *J. Geophys. Res.: Planets*, **116**, E08009, 1-15. [12] Fowler G.W. et al. (1994) *Geochim. Cosmochim. Acta*, **58**, 3921-3929. [13] Fowler G.W. et al. (1995) *Geochim. Cosmochim. Acta*, **59**, 3071-3084. [14] Mittlefehldt D.W. and Peng Z.X. (2013) *LPS 44*, Abstract #1285. [15] Ek M. et al. (2012) *LPS 43*, Abstract #2096. [16] Mittlefehldt D.W. et al. (2012) *Meteorit. Planet. Sci.*, **47**, 72-98. [17] Tkalcec B.J. and Brenker F.E. (2015) *J. Structural Geol.*, **77**, 138-150.